Use of intravascular hypo- and hyper-attenuation on non-contrast-enhanced computed tomography in diagnosing acute septic thrombophlebitis

Satoshi Yoshikawa[1*], Takeshi Ueda[1], Takuya Fujiwara[2]

1. Department of Emergency and General Internal Medicine, Rakuwakai Marutamachi Hospital, Kyoto, Japan

2. Department of Radiology, National Hospital Organization/Osaka National Hospital, Osaka, Japan

* **Correspondence:** Satoshi Yoshikawa, Department of Emergency and General Internal Medicine, Rakuwakai Marutamachi Hospital, 9-7 Jurakumawari-Matsushita-cho, Nakagyo-ku, Kyoto 604-8401, Japan
(*monimoniwo@gmail.com*)

Radiology Case. 2022 Mar; 16(3):1-14 :: DOI: 10.3941/jrcr.v16i3.4364

ABSTRACT

Septic thrombi, such as those observed in pylephlebitis and Lemierre's syndrome, are characterized by portal vein thrombosis and venous thrombosis with bacterial infection. Although radiographic findings of septic thrombus on contrast-enhanced computed tomography have been well described, no report has described the characteristics of non-contrast-enhanced computed tomography. We describe a case series of septic thrombophlebitis exhibiting intravascular hypo- and hyper-attenuation on non-contrast-enhanced computed tomography. These radiographic features reflect the pathophysiology of septic thrombus, and therefore, it is important and useful to evaluate thrombus attenuation on non-contrast-enhanced computed tomography.

CASE SERIES

CASE SERIES

Case 1

An 82-year-old woman with a two-day history of generalized fatigue and fever was admitted. Her initial vital signs were normal, except for a body temperature of 37.7°C. Her medical history included type 2 diabetes mellitus. Physical examination revealed tenderness of the right costovertebral angle. The chest X-ray (CXR) was unremarkable (Figure 1). Non-contrast-enhanced computed tomography (NECT) performed on admission day 3 revealed hypo- and hyper-attenuated regions in the superior mesenteric vein (SMV) to the portal vein (PV), with fat stranding around the SMV (Figure 2A, B). The hypo- and hyper-attenuated regions and the aorta showed a density of 40.3, 61.3, and 52.1 Hounsfield units (HU), respectively (Figure 2C, D). A thrombus within the SMV was suspected on abdominal ultrasonography (US) coupled with Doppler (Figure 3). Contrast-enhanced computed tomography (CECT) performed on admission day 4 revealed a filling defect in the SMV to the PV, suggesting a thrombus (Figure 4). Blood culture obtained on the day of admission revealed Bacteroides fragilis. Therefore, she was diagnosed with pylephlebitis. Follow-up abdominal US performed two weeks later indicated the disappearance of the thrombus (Figure 5), and abdominal NECT obtained three weeks later demonstrated normal vascular attenuation within the SMV (Figure 6A, B).

Case 2

A 70-year-old man visited the hospital with a three-week history of generalized fatigue and fever. He had a medical history of diabetes mellitus. His body temperature was 38.0°C. The right upper quadrant of the abdomen was tender, but the rest of his physical examination yielded normal results. CXR was unremarkable (Figure 7). Dynamic CECT of the abdomen obtained on the day of admission demonstrated hypo- and hyper-attenuation in the plain phase and a filling defect in the portal phase from the SMV to the PV (Figure 8A, B), with hepatic hilar lymphadenopathy. The hypo- and hyper-attenuation areas and the aorta showed a density of 22.0, 58.1, and 48.7 HU (Figure 8C, D). An abdominal US showed thrombus within the portal vein (Figure 9). Blood culture revealed Bacteroides fragilis and pylephlebitis was diagnosed. On magnetic resonance images (MRI) obtained one week after admission demonstrated absence of normal flow void within the portal vein on T2-weighted images (T2WI) and high signal intensity in the portal vein on diffusion-weighted imaging (DWI) (Figure 10A, B). The thrombus disappeared on follow-up abdominal US performed three weeks later (Figure 11).

Case 3

A 24-year-old man visited the emergency room with a one-week history of fever and sore throat. He had flu-like symptoms 2 weeks prior to presentation. Although it had improved spontaneously, he had chills with rigor just 2 hours before the visit. His body temperature was 39.4°C. Physical examination revealed tenderness of the left neck along the left internal jugular vein's (IJV) course. CXR showed multiple lung nodules in the right lung with ground-glass opacity in the left lung (Figure 12). NECT demonstrated proximal hypo-attenuation with peritonsillar abscess and peripheral hyper-attenuation in the left IJV (Figure 13A, B, C). The hypo- and hyper-attenuated regions and the right IJV showed a density of 40.1, 71.0, and 54.9 HU, respectively (Figure 13D, E). CECT revealed a thrombus in the left IJV and multiple cavitated nodules in the bilateral lungs with pulmonary infiltrates (Figure 14A, B, C). The blood culture revealed Fusobacterium necrophorum; therefore, he was diagnosed with Lemierre's syndrome. Follow-up CT and US were not performed. The patient was treated with antibiotics and discharged on admission day 24.

DISCUSSION

Etiology & Demographics:

Primary infection near the vessels can cause septic thrombophlebitis, such as pylephlebitis and Lemierre's syndrome, in which septic thrombi are observed in the portal vein and IJV [1-3]. The incidence of pylephlebitis is unknown, and it can occur across a wide age range with no sex predilection [4]. Lemierre's syndrome has an incidence of 3.6 per million people [5]. Lemierre's syndrome is more common in young adults [5] and has been reported to occur more often in men [6]. The mortality of pylephlebitis is reported to be 11% [7] to 32% [2] and that of Lemierre's syndrome is reported to be 6.4% [3]. CECT findings of septic thrombus, including a filling defect in the vessels, have been well described. However, this finding is insufficient to differentiate between a septic thrombus and a thrombus without bacterial infection.

Clinical & Imaging Findings:

Although many reports have described a filling defect in the vein observed through CECT in cases of septic thrombi, such as in pylephlebitis and Lemierre's syndrome, no report has described the characteristics of septic thrombi on NECT.

According to a study assessing CT values of blood phantom, hematocrit and hemoglobin are linearly correlated with CT values [8]. This is because the CT values of blood can be attributed to the density of hemoglobin within RBCs, which accounts for 95% or more of the blood cells.

On the other hand, portal vein thrombosis [9], cerebral sinus thrombosis [10,11], and pulmonary thromboembolism [12] show hyper-attenuation within the vessels on NECT. Furthermore, the attenuation of acute thrombus is not dependent on the hematocrit because the density of thrombus depends on its intrinsic structure without serum rather than on the rheological property of circulating blood [12]; therefore, acute thrombus normally exhibits higher attenuation than circulating blood in the vessels.

In contrast to acute thrombus, an acute septic thrombus may show hypo-attenuation because it contains many bacteria and neutrophils [13]. Neutrophil infiltration induces inflammation with fluids, which may also contribute to the hypo-attenuation shown by septic thrombi. In fact, the thrombi demonstrated partial hypo- and hyper-attenuation in all the current cases, suggesting acute thrombi with and without neutrophil infiltration, respectively. However, severe anemia may obscure the difference in attenuation between a septic thrombus and circulating blood. The attenuation of circulating blood in patients with severe anemia decreases as hematocrit and hemoglobin are linearly correlated with CT values. A 5.2 g/dL of hemoglobin phantom exhibited an attenuation of 32.5 to 39.8 HU [8], which are similar to the CT values of the septic thrombus in cases 1 and 3. In such cases, a septic thrombus may not be detected on NECT.

Treatment & Prognosis:

Septic thrombophlebitis should be treated with appropriate antibiotics and the typical duration of antibiotic therapy is at least four to six weeks [2]. Although some case reports have described the efficacy of anticoagulant therapy in Lemierre's syndrome [14], it is uncertain if anticoagulants prevent thrombus propagation and extension.

Differential Diagnosis:

Although septic thrombus shows hypo-attenuation because of abundant bacteria and neutrophils, some other pathological conditions also exhibit hypo-attenuation in the vessels if they contain fibrin, abscess, necrotic tissue, and fluid.

Chronic thrombus

Chronic thrombus could show hypo-attenuation relative to the blood as well as to septic thrombus. The attenuation of the thrombus gradually decreases for 7-14 days [15], almost

exhibiting iso-attenuation with normal blood, and chronic thrombus could exhibit hypo-attenuation relative to circulating blood [12]. A report described that even a subacute thrombus can show hypo-attenuation [16] because of rapid thrombus evolution, in which the proportion of high-density red blood cells decreases and that of low-density fibrin increases [12,17]. Although chronic thrombus may be a differential diagnosis of septic thrombus because both thrombi show hypo-attenuation, partial hyper-attenuation supports a diagnosis of septic thrombus, except for acute-on-chronic thrombus. Moreover, it may be easy to differentiate according to the history of the presenting illness, evidence of inflammation, positive blood culture, and fat stranding around the vessel.

Intravascular abscess

We encountered a case of intravascular abscess in which hypo-attenuation similar to water density within the vessels was detected on NECT. A patient presented with a hepatic caudal lobe abscess that ruptureds into the retroperitoneal cavity (Figure 15A, B, C). Percutaneous retroperitoneal abscess drainage was performed because percutaneous hepatic caudal lobe abscess drainage was technically difficult (Figure 15D). Follow-up abdominal CT indicated improvement of the retroperitoneal abscess with hypo-attenuation within the inferior vena cava (IVC) on NECT and a filling defect on CECT (Figure 16A, B). The filling defect was floating balloon shaped on coronal CECT (Figure 17A), suggesting intravascular abscess rather than a septic thrombus. Consequently, an abcessogram, in which contrast media was injected through the drainage tube, was performed. An abcessogram demonstrated an abscess floating within the IVC; therefore, we diagnosed an abscess penetrating into the IVC (Figure 17B). Although an intravascular abscess is extremely rare, it is difficult to distinguish it from septic thrombus.

Tumor invasion

In a case of intravascular tumor invasion with necrosis, the patient presented with undifferentiated thyroid carcinoma with a hypo-attenuating left IJV on NECT (Figure 18A). CECT revealed heterogenous enhancement in the left IJV, necrotic foci in the thyroid tumor, enlarged lymph nodes (Figure 18B), and multiple lung nodules. Fine-needle aspiration revealed neutrophils without tumor cells and bacteria. The aspirate and blood cultures were negative. The patient rapidly deteriorated and died 2 weeks later despite antibiotic administration, and undifferentiated thyroid carcinoma invading the IJV was diagnosed.

Pancreatic pseudocyst invasion

We encountered a case of pancreatic pseudocyst penetrating into the splenic vein. NECT demonstrated hypo-attenuation similar to water density within the splenic vein (Figure 19A). Magnetic resonance imaging with cholangiopancreatography (MRCP) revealed a T2-weighted hyperintense cystic lesion that was continuous with the main pancreatic duct and splenic vein (Figure 19B). These findings were consistent with pancreatic pseudocyst penetrating into the splenic vein and left-sided portal hypertension. Therefore, hypo-attenuation within the vessels does not always suggest a thrombus.

In conclusion, our three patients presenting with septic thrombophlebitis showed intravascular hypo- and hyper-attenuation on NECT, which reflected the pathophysiology of the thrombi. This case series reinforces that awareness regarding the importance of evaluating thrombus on NECT is necessary among radiologists.

TEACHING POINT

Patients with a septic thrombus often present with non-specific symptoms. Evaluation of hypo- and hyper-attenuation in a thrombus on non-contrast-enhanced computed tomography may be useful to detect a septic thrombus; therefore, although a thrombus is often evaluated on contrast-enhanced computed tomography, it is important to evaluate thrombus attenuation on non-contrast-enhanced computed tomography as a first imaging examination for diagnosis.

REFERENCES

1. Kasper DL, Sahani D, Misdraji J. Case records of the Massachusetts General Hospital. Case 25-2005. A 40-year-old man with prolonged fever and weight loss. N Engl J Med. 2005 Aug;353(7):713-2. PMID: 16107625.

2. Plemmons RM, Dooley DP, Longfield RN. Septic thrombophlebitis of the portal vein (pylephlebitis): diagnosis and management in the modern era. Clin Infect Dis. 1995 Nov;21(5):1114-20. PMID: 8589130.

3. Chirinos JA, Lichtstein DM, Garcia J, Tamariz LJ. The evolution of Lemierre syndrome: report of 2 cases and review of the literature. Medicine (Baltimore). 2002 Nov;81(6):458-65. PMID: 12441902.

4. Kanellopoulou T, Alexopoulou A, Theodossiades G, Koskinas J, Archimandritis AJ. Pylephlebitis: an overview of non-cirrhotic cases and factors related to outcome. Scand J Infect Dis. 2010 Dec;42(11-12):804-11. PMID: 20735334.

5. Hagelskjaer Kristensen L, Prag J. Lemierre's syndrome and other disseminated Fusobacterium necrophorum infections in Denmark: a prospective epidemiological and clinical survey. Eur J Clin Microbiol Infect Dis. 2008 Sep;27(9):779-89. PMID: 18330604.

6. Brazier JS, Hall V, Yusuf E, Duerden BI. Fusobacterium necrophorum infections in England and Wales 1990-2000. J Med Microbiol. 2002 Mar;51(3):269-72. PMID: 11871622.

7. Choudhry AJ, Baghdadi YM, Amr MA, Alzghari MJ, Jenkins DH, Zielinski MD. Pylephlebitis: a Review of 95 Cases. J Gastrointest Surg. 2016 Mar;20(3):656-661. PMID: 26160320.

8. Okada T. The relation between CT value of blood and red blood corpuscle (RBC), hematocrit (Hct), hemoglobin (Hb) and Attempt of calculation for Hct value from CT images. EPOS Poster ECR 2011/C-1445. https://epos.myesr.org/poster/esr/ecr2011/C-1445. Accessed October 18, 2021. doi: 10.1594/ecr2011/C-1445

9. Mori H, Hayashi K, Uetani M, Matsuoka Y, Iwao M, Maeda H. High-attenuation recent thrombus of the portal vein: CT demonstration and clinical significance. Radiology 1987 May;163(2):353-356. PMID: 3031725.

10. Black DF, Rad AE, Gray LA, Campeau NG, Kallmes DF. Cerebral venous sinus density on noncontrast CT correlates with hematocrit. Am J Neuroradiol. 2011 Aug;32(7):1354-7. PMID: 21566009.

11. Buyck PJ, De Keyzer F, Vanneste D, Wilms G, Thijs V, Demaerel P. CT density measurement and H: H ratio are useful in diagnosing acute cerebral venous sinus thrombosis. Am J Neuroradiol. 2013 Aug;34(8):1568-72. PMID: 23471024.

12. De Luca F, Modolon C, Buia F, et al. Densitometric CT evaluation of acute and chronic thromboembolic filling defects of the pulmonary arteries before and after contrast injection. Radiol Med. 2012 Sep;117(6):979-991. PMID: 22580809.

13. Hubbard E, Wise E, Hubbard B, Girard S, Kong B, Moudgal V. Tucked Away: An Infected Thrombus. Am J Med. 2016 Jun;129(6):576-9. PMID: 26901112.

14. Phua CK, Chadachan VM, Acharya R. Lemierre syndrome-should we anticoagulate? A case report and review of the literature. Int J Angiol. 2013 Jun;22(2):137-42. PMID: 24436600.

15. Virapongse C, Cazenave C, Quisling R, Sarwar M, Hunter S. The empty delta sign: frequency and significance in 76 cases of dural sinus thrombosis. Radiology. 1987 Mar;162(3):779-85. PMID: 3809494.

16. Neal E, Sturgeon J. Hypodense cerebral venous sinus thrombosis on unenhanced CT: A potential pitfall. Report of a case and review of the literature. Radiol Case Rep. 2019 Nov;15(1):35-8. PMID: 31737143.

17. Kirchhof K, Welzel T, Mecke C, Zoubaa S, Sartor K. Differentiation of white, mixed, and red thrombi: value of CT in estimation of the prognosis of thrombolysis phantom study. Radiology. 2003 Jul;228(1):126-130. PMID: 12728185.

FIGURES

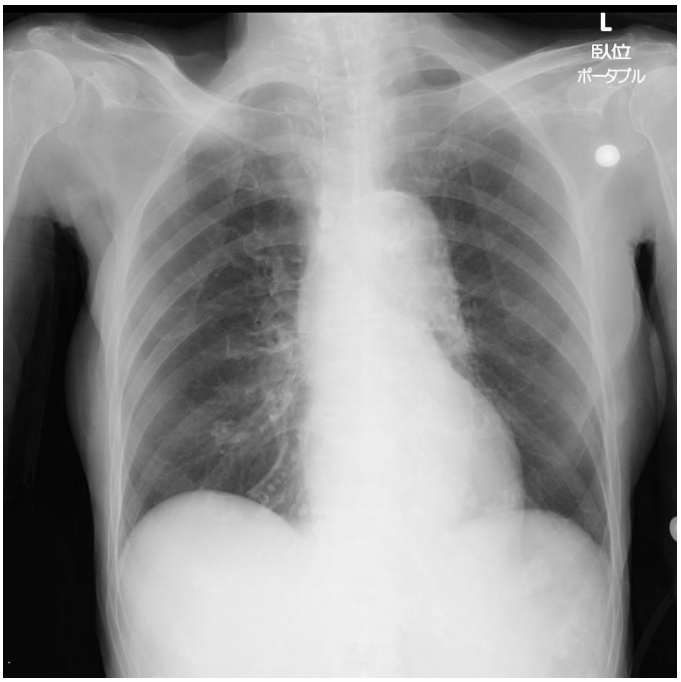

Figure 1: 82-year-old woman with pylephlebitis

FINDINGS: No abnormal findings are detected.

TECHNIQUE: The supine anteroposterior chest view acquired at 120 kV and 5 mAs.

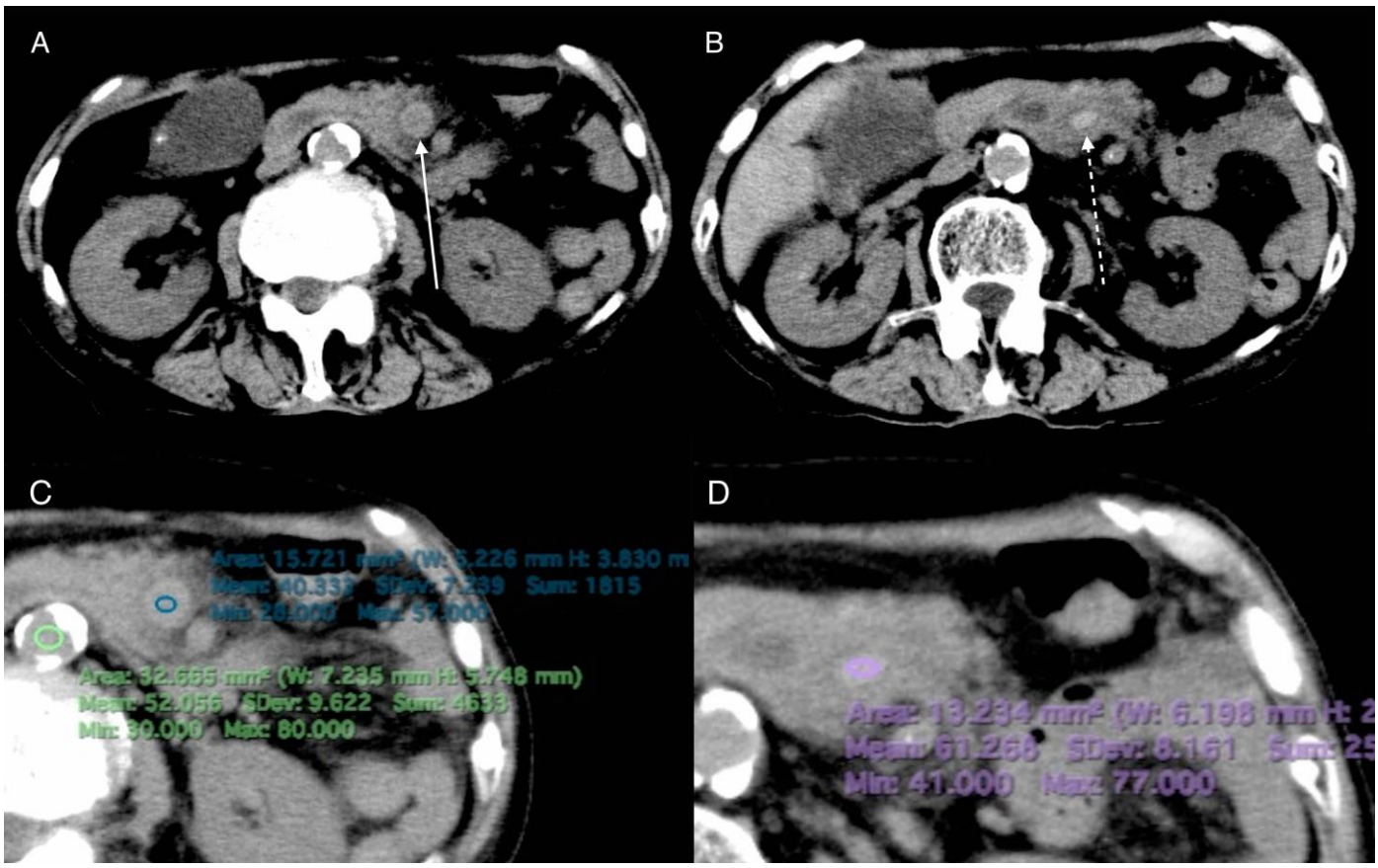

Figure 2: 82-year-old woman with pylephlebitis

FINDINGS: Axial NECT shows intravascular hypo- (A arrow) and hyper-attenuation (B dashed arrow) in the peripheral and central SMV, respectively. The intravascular hypo- and hyper-attenuation, and the aorta show 40.3, 61.3, and 52.1 HU, respectively (C,D).

TECHNIQUE: Non-enhanced axial CT images were acquired with TOSHIBA Aquilion 16-slices CT scanner at 93 mAs, 120 kV, and 8 mm slice thickness.

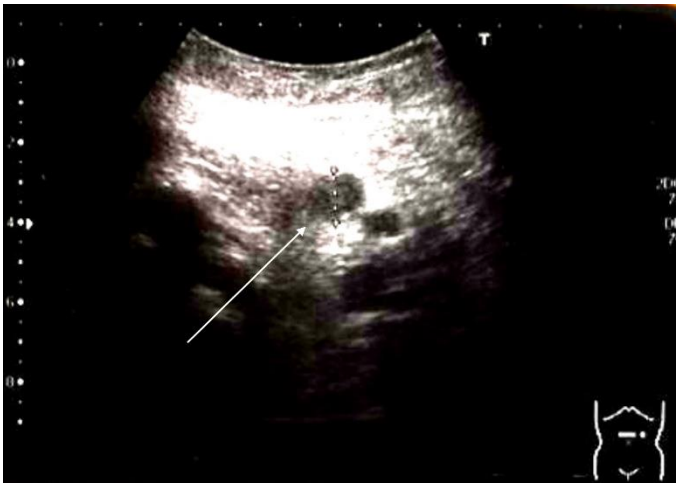

Figure 3: 82-year-old woman with pylephlebitis

FINDINGS: Gray-scale image from the US study shows an echogenic thrombus in the SMV (arrow).

TECHNIQUE: TOSHIBA Aplio MX, convex probe, 4.0 MHz.

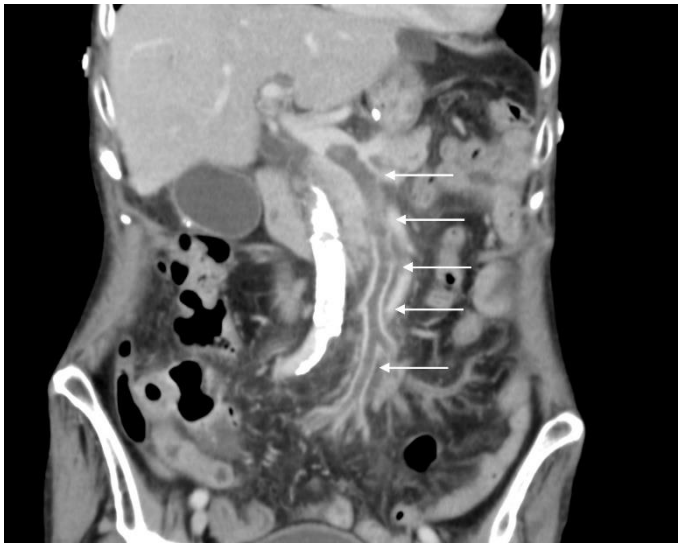

Figure 4: 82-year-old woman with pylephlebitis

FINDINGS: Coronal CECT demonstrates a filling defect within the SMV to PV (arrows), suggesting a thrombus. Pylephlebitis was diagnosed after the positive result of blood culture.

TECHNIQUE: Coronal CECT with multiplanar reformats. Images were acquired with TOSHIBA Aquilion 16-slices CT scanner at 97 mAs, 120 kV, and 4 mm slice thickness after intravenous administration of 100 mL of Iopamidol (Iopamidol) 300 mg iodine/mL.

Figure 5 (right): 82-year-old woman with pylephlebitis

FINDINGS: The echogenic thrombus in the SMV disappeared on gray-scale image from the US study (arrow).

TECHNIQUE: TOSHIBA Aplio MX, convex probe, 4.0 MHz.

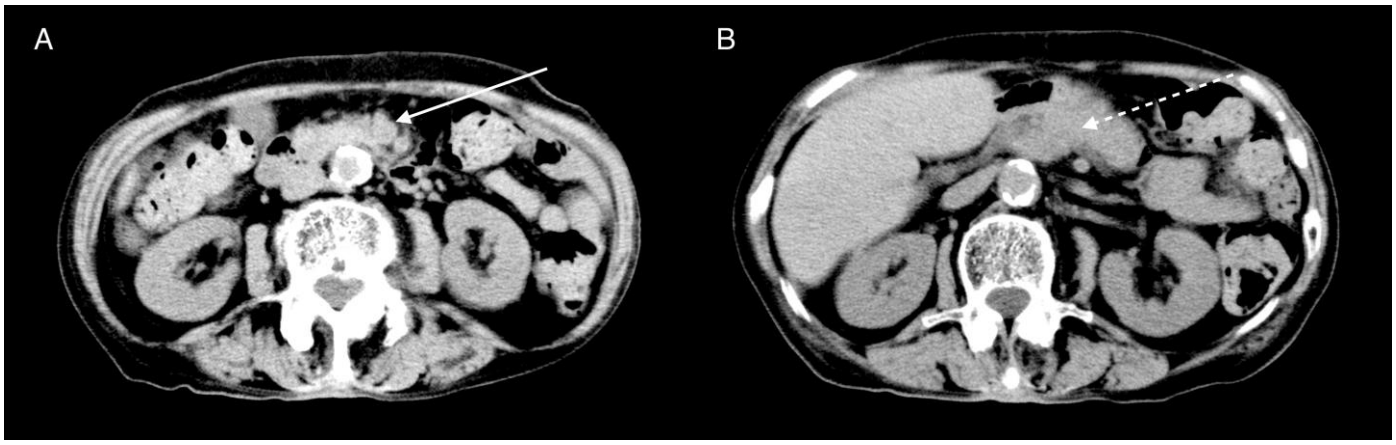

Figure 6: 82-year-old woman with pylephlebitis

FINDINGS: Axial NECT obtained three weeks after admission shows normal attenuation within the SMV (A arrow, B dashed arrow).

TECHNIQUE: Non-enhanced axial CT images were acquired with TOSHIBA Aquilion 16-slices CT scanner at 57 mAs, 120 kV, and 8 mm slice thickness.

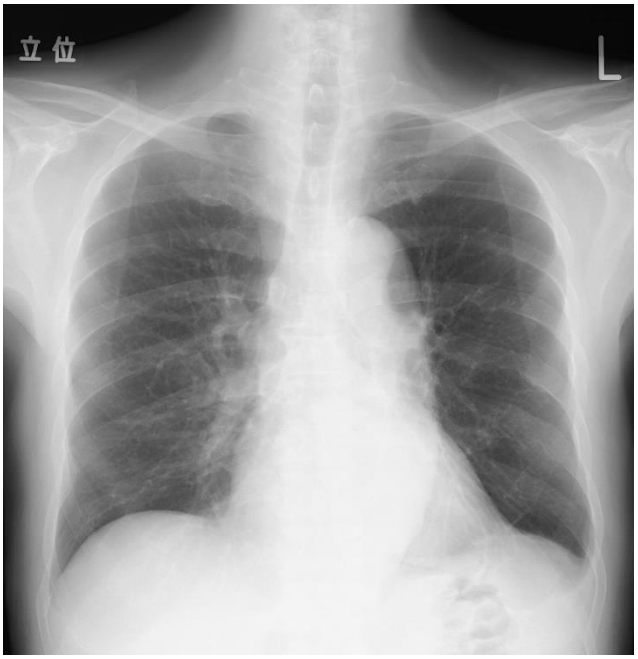

Figure 7 (right): 70-year-old man with pylephlebitis

FINDINGS: No abnormal findings are detected.

TECHNIQUE: The posteroanterior chest view acquired at 120 kV and 5 mAs.

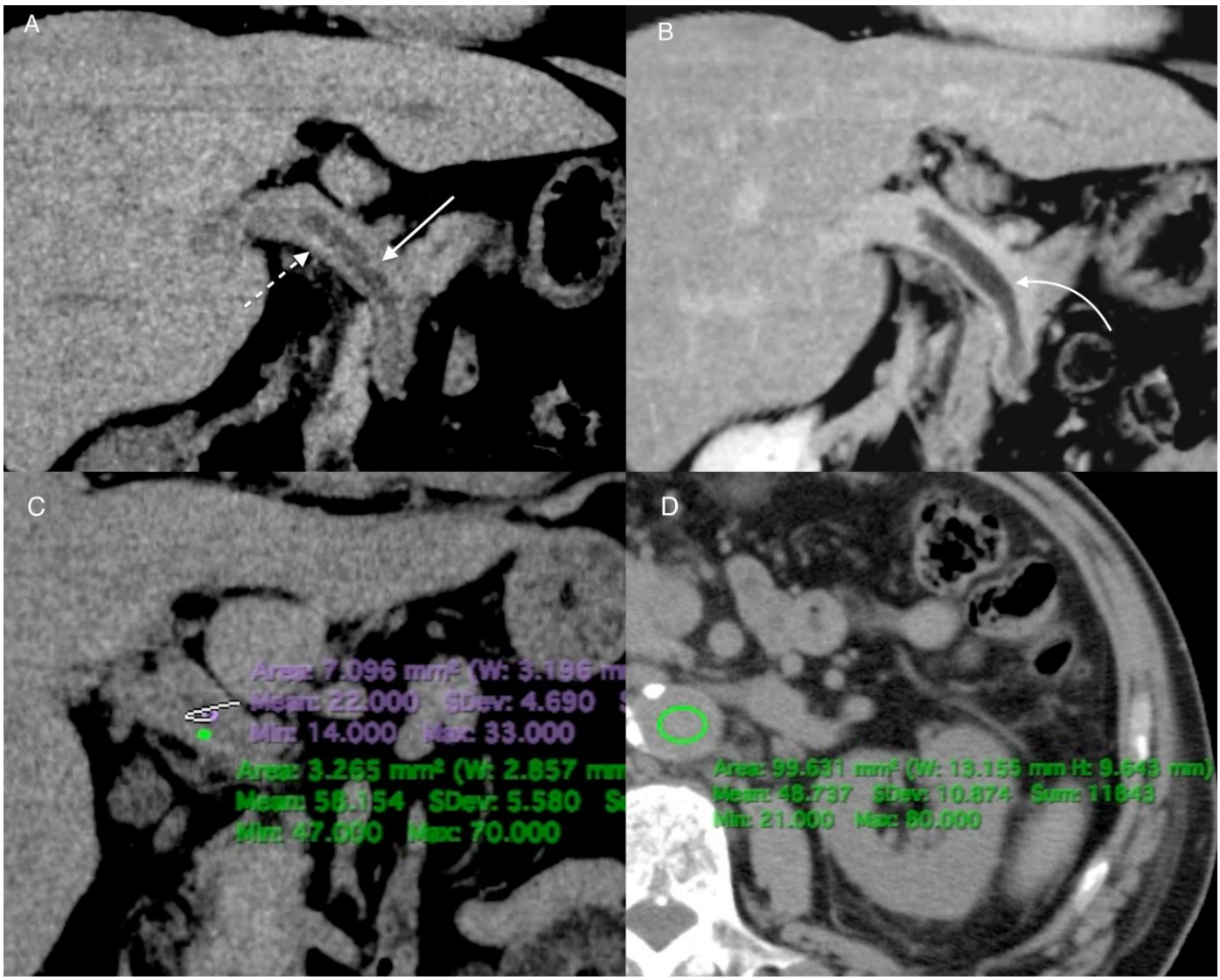

Figure 8: 70-year-old man with pylephlebitis

FINDINGS: Coronal reformatted images of dynamic CECT demonstrate portal hypo- (A arrow) and hyper-attenuation (A dashed arrow) in the plain phase and a filling defect in the portal phase within the SMV to PV (B curved arrow). In the plain phase hypo- and hyper-attenuation, and the aorta show 22.0, 58.1 on coronal CT, and 48.7 HU on axial CT, respectively (C, D).

TECHNIQUE: Coronal and Axial dynamic CECT with multiplanar reformats. Images were acquired with TOSHIBA Aquilion 16-slices CT scanner at 163 mAs for A, C, and D, 105 mAs for B, 120 kV, and 3 mm slice thickness after intravenous administration of 100 mL of Iopamidol (Iopamidol) 300 mg iodine/mL.

Figure 9: 70-year-old man with pylephlebitis

FINDINGS: Gray-scale image from the US study demonstrates an echogenic thrombus in the portal vein (arrow).

TECHNIQUE: TOSHIBA Aplio MX, convex probe, 4.0 MHz.

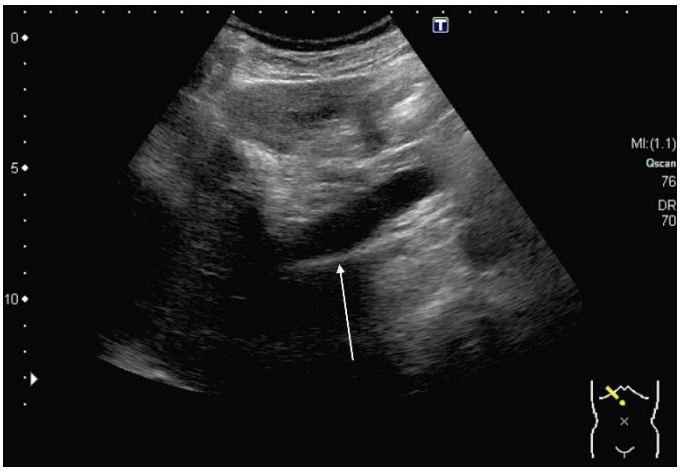

Figure 11: 70-year-old man with pylephlebitis

FINDINGS: The thrombus in the portal vein disappeared on gray-scale US image.

TECHNIQUE: TOSHIBA Aplio MX, convex probe, 4.0 MHz.

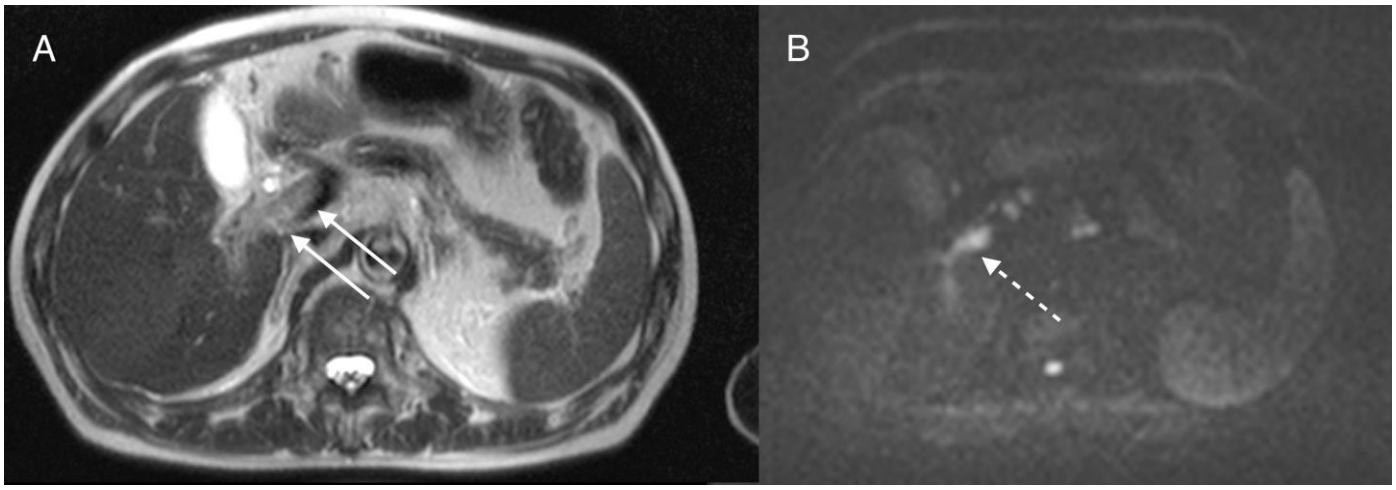

Figure 10: 70-year-old man with pylephlebitis

FINDINGS: Axial MRI reveals absence of normal flow void on T2WI (A arrows) and hyperintensity on DWI within the portal vein (B dashed arrow).

TECHNIQUE: Axial T2WI was performed using a SIEMENS Symphony 1.5T MRI scanner with a TE: 108, TR: 950, axial DWI was performed with a TE: 76, TR: 5300, B-value: 800.

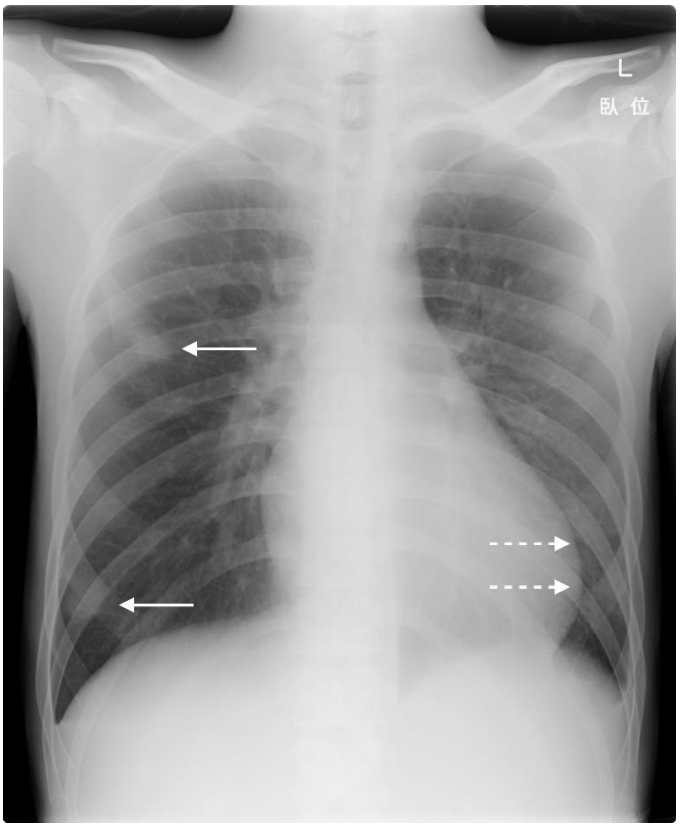

Figure 12 (left): 24-year-old man with Lemierre's syndrome

FINDINGS: CXR shows multiple lung nodules in the right lung (arrows) with ground-glass opacity in the left lung (dashed arrows).

TECHNIQUE: The posteroanterior chest view acquired at 120 kV and 5 mAs.

Figure 13 (bottom): 24-year-old man with Lemierre's syndrome

FINDINGS: Axial NECT of the neck with multiplanar reformats demonstrates left internal jugular hypo-attenuation proximally (A, C arrows) with peritonsillar abscess (B curved arrow) and hyper-attenuation peripherally (B, C dashed arrows) showing 40.1 and 71.0 HU, respectively, while the right IJV shows 54.9 HU (D, E).

TECHNIQUE: Non-enhanced axial CT with multiplanar reformats. Images were acquired with TOSHIBA Aquilion 16-slices CT scanner at 225 mAs, 120 kV, and 5 mm slice thickness.

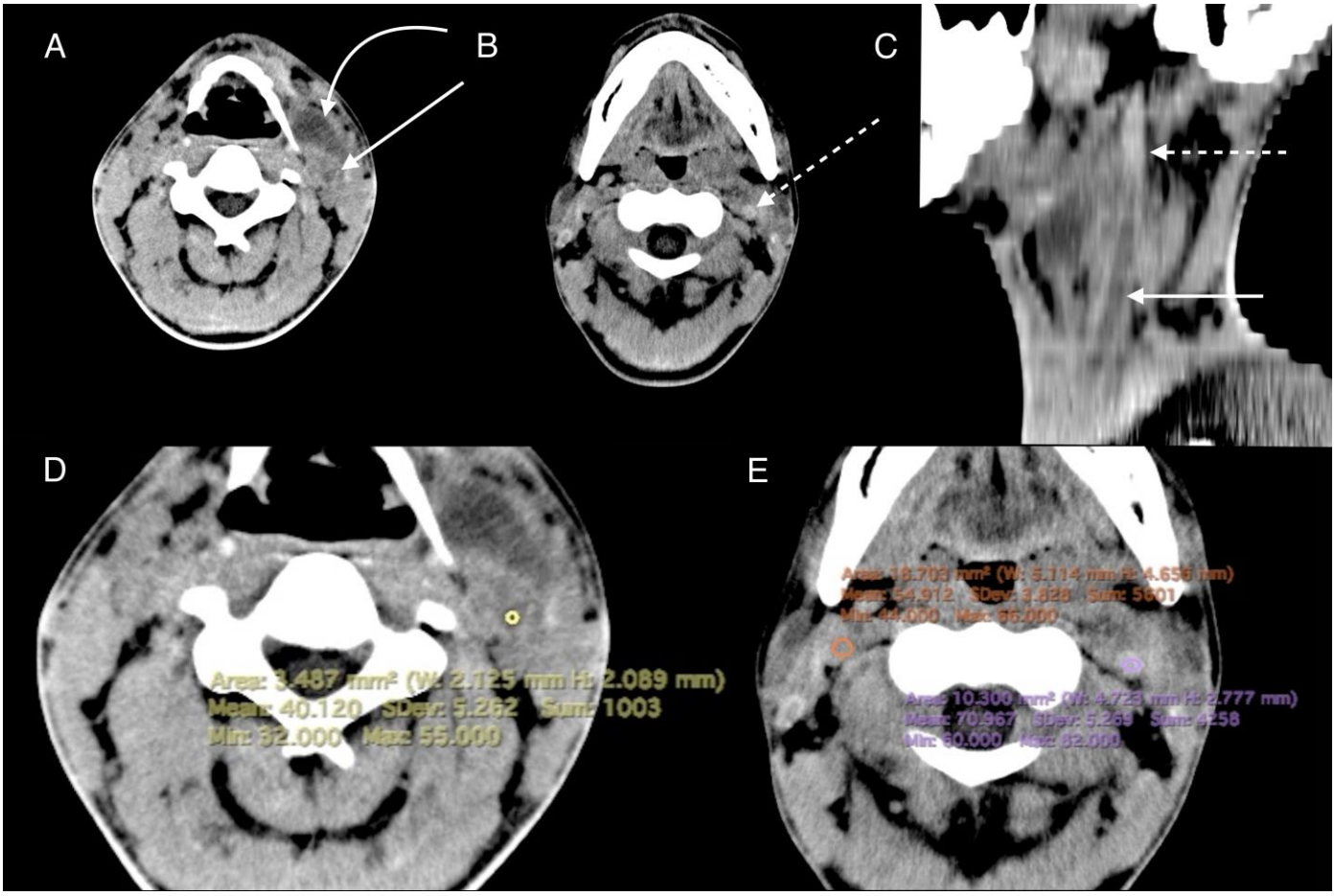

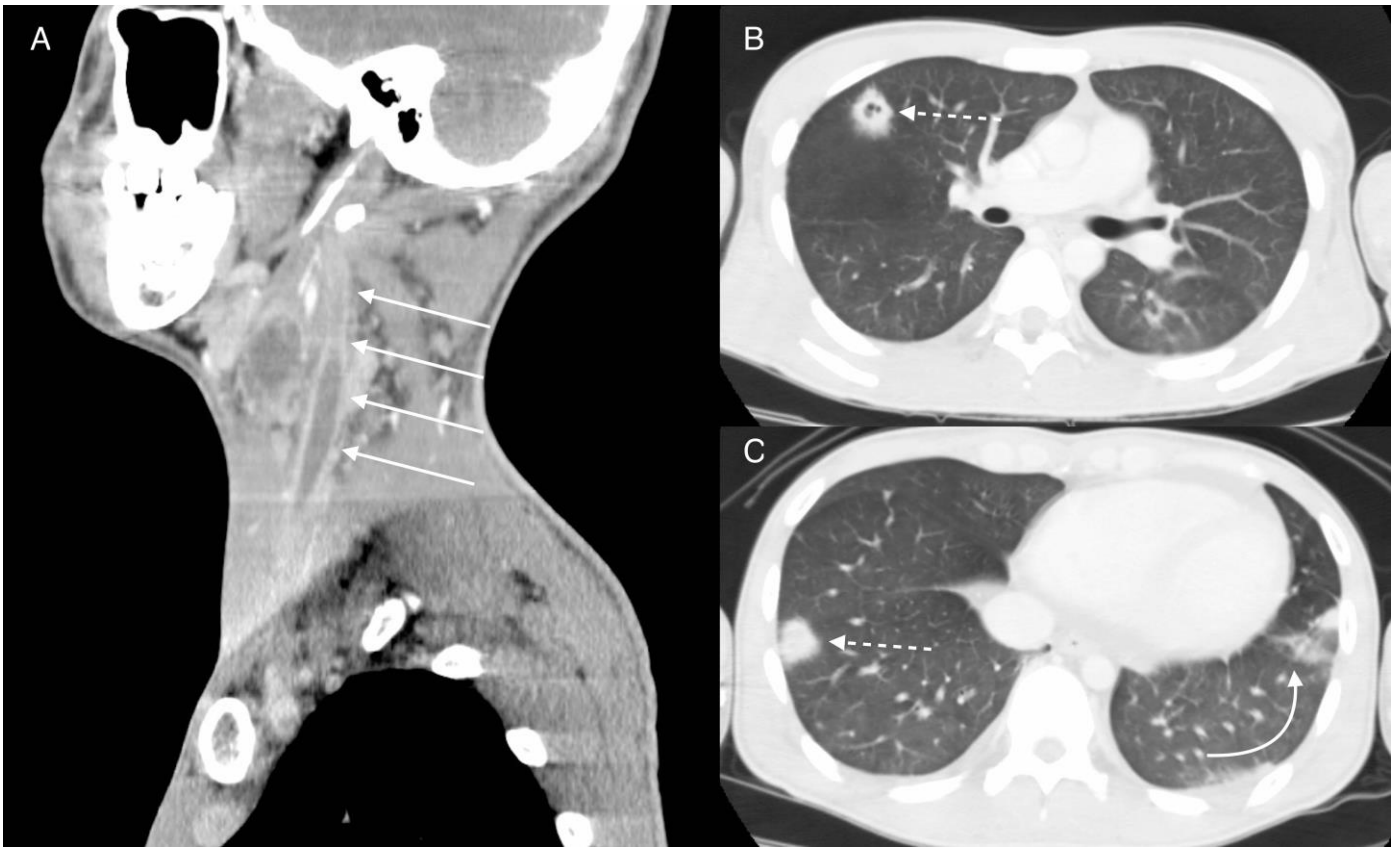

Figure 14: 24-year-old man with Lemierre's syndrome

FINDINGS: Axial CECT with multiplanar reformats shows a filling defect in the left IJV (A arrows) and multiple cavitated nodules (B, C dashed arrows) with pulmonary infiltrates (C curved arrow)

TECHNIQUE: Axial CECT with multiplanar reformats. Images were acquired with TOSHIBA Aquilion 16-slices CT scanner at 75 mAs, 120 kV, and 5 mm slice thickness after intravenous administration of 100 mL of Iopamidol (Iopamidol) 300 mg iodine/mL.

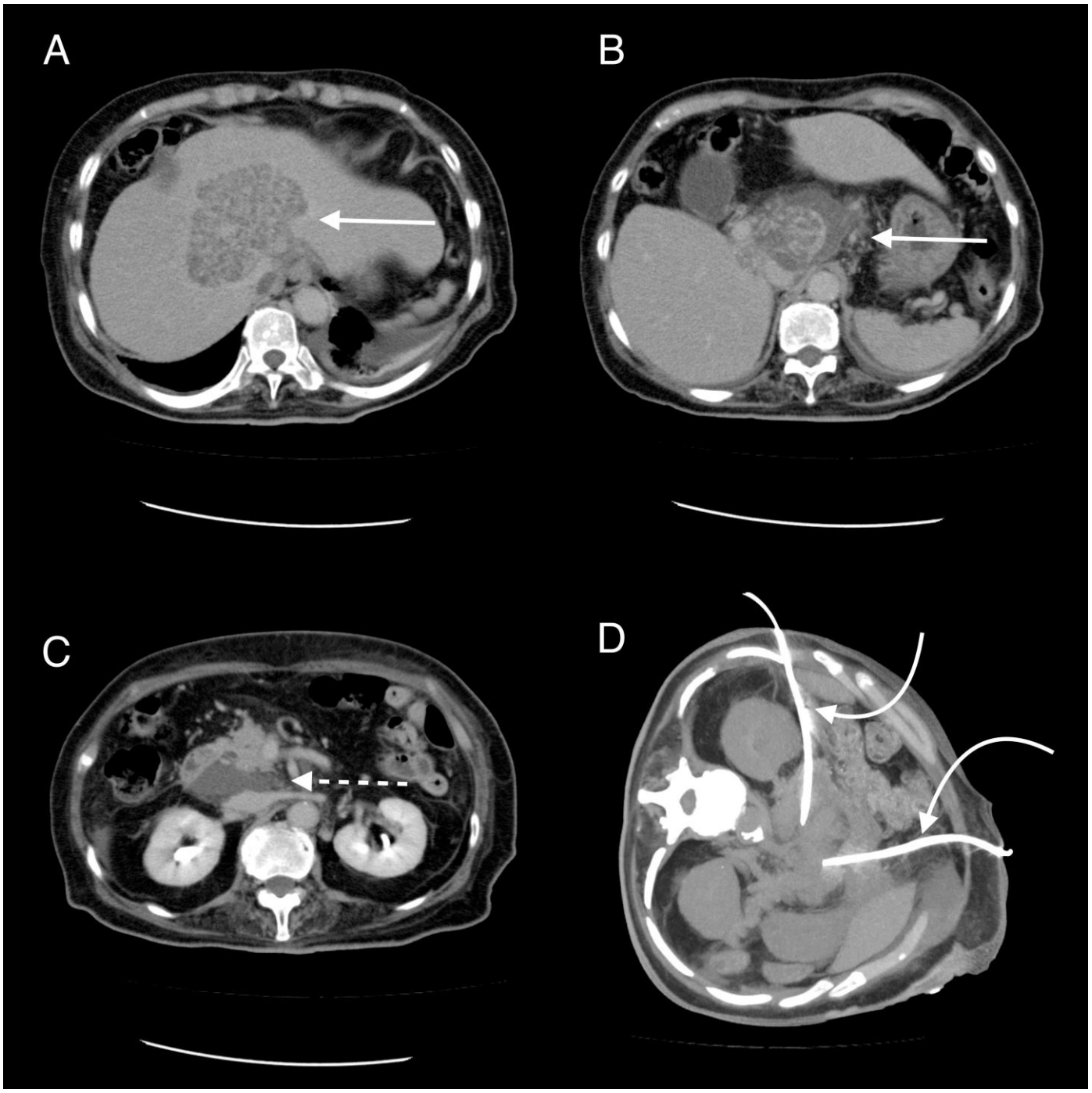

Figure 15: 92-year-old woman with a hepatic caudal lobe abscess penetrating into the retroperitoneal cavity.

FINDINGS: Axial CECT demonstrates a hepatic caudal lobe abscess with rupture (A, B arrows) penetrating into the retroperitoneal space (C dashed arrow). Axial CT-guided percutaneous drainage for retroperitoneal abscess was performed (D curved arrows).

TECHNIQUE: Axial CECT. Images were acquired with TOSHIBA Aquilion 16-slices CT scanner at 171 mAs, 120 kV, and 5 mm slice thickness after intravenous administration of 100 mL Iopamidol (Iopamidol) 300 mg iodine/mL (A, B, and C). Axial 31 mm maximum intensity projection image of CT-guided percutaneous drainage. TOSHIBA Aquilion 16-slices CT scanner at 200 mAs and 120 kV (D).

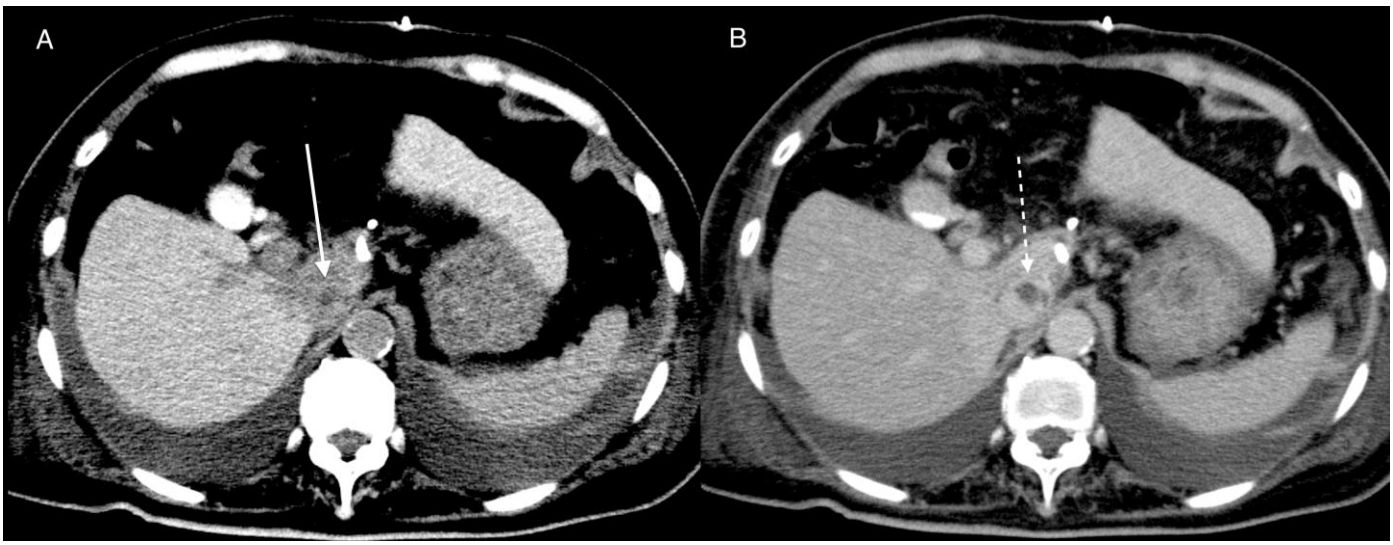

Figure 16: 92-year-old woman with a hepatic caudal lobe abscess penetrating into the IVC

FINDINGS: Axial NECT demonstrates hypo-attenuation similar to water density within the IVC (A arrow). Axial CECT shows a filling defect in the venous phase (B dashed arrow).

TECHNIQUE: Axial NECT. TOSHIBA Aquilion 16-slices CT scanner at 171 mAs, 120 kV, and 5 mm slice (A). Axial CECT. TOSHIBA Aquilion 16-slices CT scanner at 172 mAs, 120 kV, and 5 mm slice thickness after intravenous administration of 100 mL Iopamidol (Iopamidol) 300 mg iodine/mL (B).

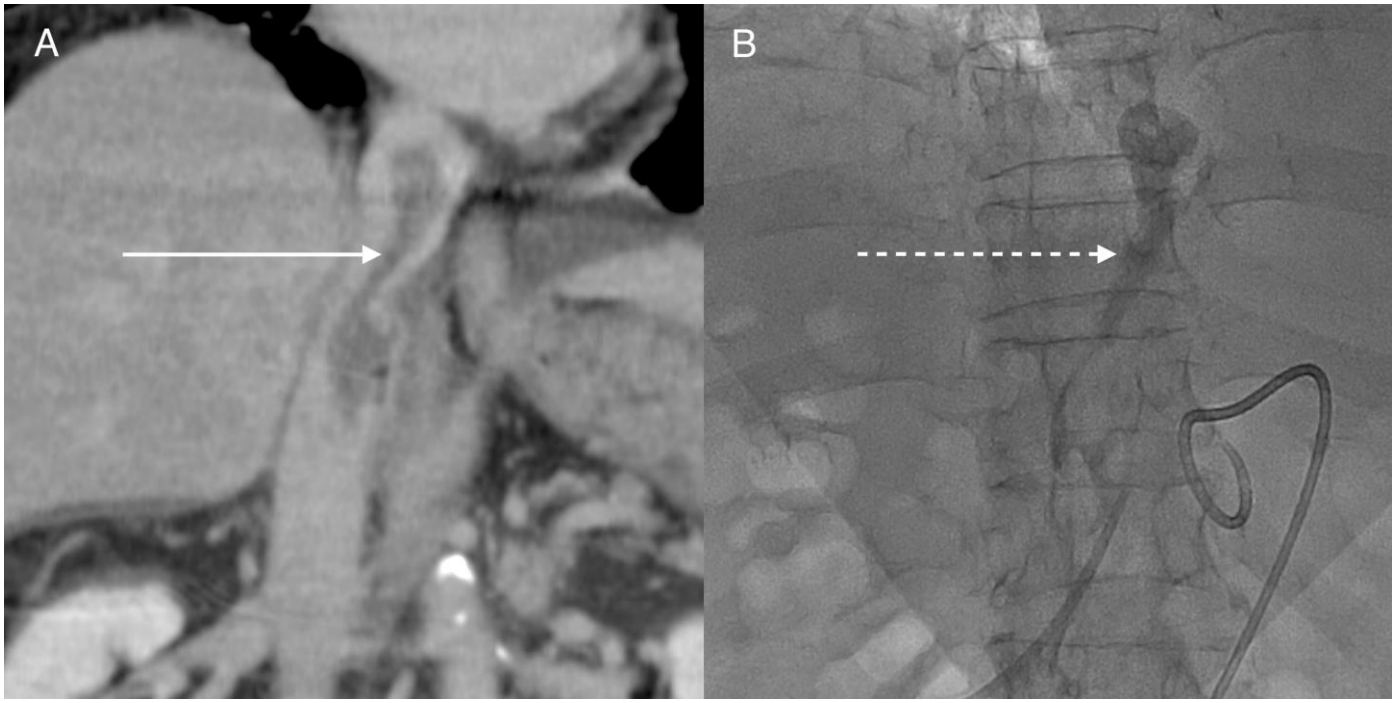

Figure 17: 92-year-old woman with a hepatic caudal lobe abscess penetrating into the IVC

FINDINGS: Coronal CECT demonstrates floating balloon shaped hypo-attenuation, which favors intravascular abscess over a septic thrombus (A arrow). An abscessogram shows an abcess floating in the IVC (B dashed arrow).

TECHNIQUE: Coronal CECT. Images were acquired with TOSHIBA Aquilion 16-slices CT scanner at 172 mAs, 120 kV, and 5 mm slice thickness after intravenous administration of 100 mL Iopamidol (Iopamidol) 300 mg iodine/mL (A). An abcessogram after administration of 10ml of Amidotrizoic Acid (Urografin injection 60%) 292 mg iodine/mL through drainage tube (B).

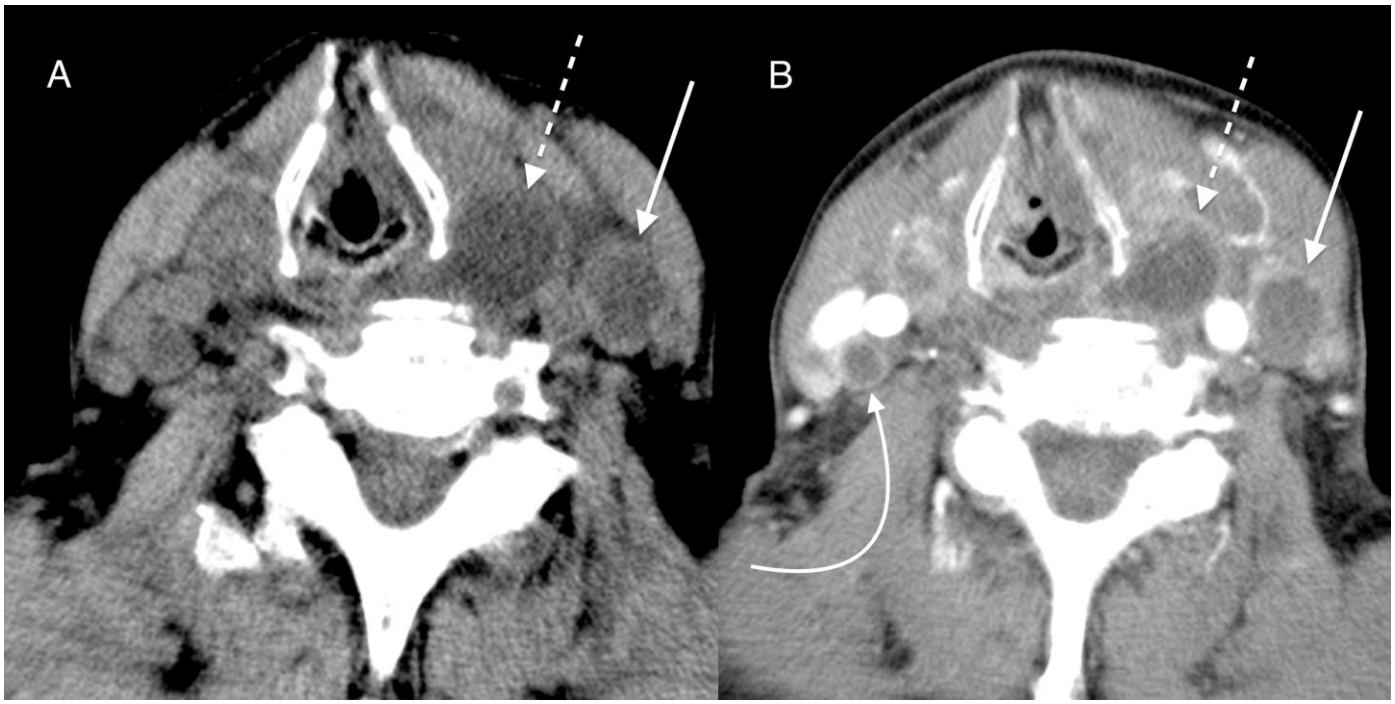

Figure 18: 88-year-old woman with undifferentiated thyroid carcinoma with left IJV

FINDINGS: Hypo-attenuation in the left IJV and thyroid tumor are demonstrated on axial NECT (A arrow, dashed arrow) and axial CECT (B arrow, dashed arrow). Axial CECT also shows enlarged lymph nodes with necrotic foci (B curved arrow).

TECHNIQUE: Axial NECT and CECT. Images were acquired with TOSHIBA Aquilion 16-slices CT scanner at 35 mAs, for A and 34 mAs for B, 120 kV, and 5 mm slice thickness after intravenous administration of 100 mL Iopamidol (Iopamidol) 300 mg iodine/mL.

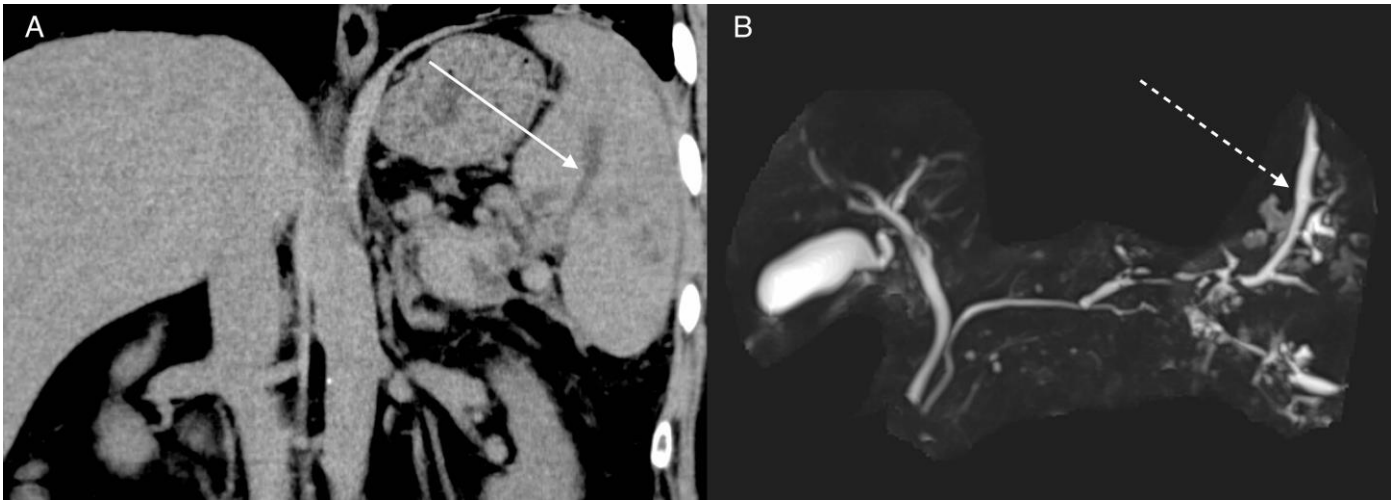

Figure 19: 46-year-old man with pancreatic pseudocyst penetrating into the splenic vein

FINDINGS: Coronal NECT demonstrates hypo-attenuation similar to water density within the splenic vein (A arrow). 3D MRCP reveals a T2-weighted hyperintense lesion within the splenic vein (B dashed arrow) that has a continuity with the main pancreatic duct.

TECHNIQUE: Coronal NECT. Images were acquired with TOSHIBA Aquilion 16-slices CT scanner at 171 mAs, 120 kV, and 5 mm slice thickness. 3D MRCP was performed using a SIEMENS Verio 3T MRI scanner with a TE: 716, TR: 5415 after oral ingestion of manganese chloride tetrahydrate (Bothdel Oral Solution 10).

Etiology	The organ infection near the vessels and thrombophlebitis of small veins lead to septic thrombophlebitis.
Prevalence	Pylephlebitis: unknown. Lemierre's syndrome: 3.6 cases per million people.
Gender ratio	Pylephlebitis: no significant difference in gender ratio. Lemierre's syndrome: men > women
Age predilection	Pylephlebitis: wide age range. Lemierre's syndrome: young adults.
Risk factors	Pylephlebitis: appendicitis, diverticulitis. Lemierre's syndrome: tonsillitis, peritonsillar infection.
Treatment	Antibiotics. It is uncertain that anticoagulants prevent thrombus propagation and extension.
Prognosis	Pylephlebitis: mortality rate is 11% to 32%. Lemierre's syndrome: mortality rate is 6.4%.
Imaging Findings	Intravascular hypo- and hyper-attenuation on non-contrast-enhanced computed tomography and a filling defect on contrast-enhanced computed tomography.

Table 1: Summary table of Pylephlebitis and Lemierre's syndrome.

	NECT	CECT	MRI
Septic thrombophlebitis	Intravascular hypo- and hyper-attenuation that represent septic thrombus and acute thrombus, respectively.	A filling defect	Absence of normal flow void on T2-weighted images, high intensity on diffusion-weighted imaging
Chronic thrombus	Intravascular hypo-attenuation.	A filling defect	Absence of normal flow void on T2-weihgted images, low to intermediate intensity on diffusion-weighted imaging
Intravascular abscess	Intravascular hypo-attenuation similar to water density.	A filling defect	Absence of normal flow void on T2-weighted images, high intensity on diffusion-weighted imaging
Tumor invasion	Mixed hypo- and hyper-attenuation that represent necrosis and viable tumor tissue, respectively.	Heterogeneous enhancement	Heterogeneous intensity on T1-weighted images, T2-weighted images, and diffusion-weighted imaging
Pancreatic pseudocyst invasion	Hypo-attenuation similar to water density.	A filling defect	T2 hyperintense similar to water intensity.

Table 2: Differential diagnosis table for septic thrombophlebitis.

ABBREVIATIONS

CECT = Contrast-enhanced computed tomography
DWI = Diffusion-weighted imaging
HU = Hounsfield units
IJV = Internal jugular vein
IVC = Inferior vena cava
MRCP = Magnetic resonance imaging with cholangiopancreatography
MRI = Magnetic resonance imaging
NECT = Non-contrast-enhanced computed tomography
PV = Portal vein
SMV = Superior mesenteric vein
T2WI = T2-weighted images

KEYWORDS

pylephlebitis; septic thrombophlebitis; venous thrombosis; portal vein thrombosis; Lemierre's syndrome

Online access
This publication is online available at:
www.radiologycases.com/index.php/radiologycases/article/view/4364

Peer discussion
Discuss this manuscript in our protected discussion forum at:
www.radiolopolis.com/forums/JRCR

Interactivity
This publication is available as an interactive article with scroll, window/level, magnify and more features.
Available online at www.RadiologyCases.com

Published by EduRad
www.EduRad.org